Desalination and Water Treatment
www.deswater.com

doi: 10.5004/dwt.2017.20454

67 (2017) 397–405
March

Tartrazine removal from water using functionalized multiwall carbon nanotubes

A. Nait-Merzoug[a,c,*], O. Guellati[a,b,d,*], A. Benjaballah[a], I. Janowska[d], D. Bégin[d], N. Manyala[e], M. Guerioune[b]

[a]*Université Mohamed Cherif Messaadia de Souk Ahras, Faculté des Sciences, B.P. 1553, 41000 Souk-Ahras, Algeria, emails: abenlala@yahoo.fr (A. Nait-Merzoug), guellati23@yahoo.fr (O. Guellati), assia_bendjaballah@yahoo.com (A. Benjaballah)*
[b]*Laboratoire d'Etude et de Recherche des Etats Condensés (LEREC), Département de Physique, Université Badji-Mokhtar de Annaba, B.P. 12, 23000 Annaba, Algeria, email: mguerioune@yahoo.fr*
[c]*Laboratoire des Science et Techniques de l'eau et d'environnement, Université Mohamed Cherif Messaadia de Souk Ahras, B.P. 1553, 41000 Souk-Ahras, Algeria*
[d]*Institut de Chimie et Procédés pour l'Energie, l'Environnement et la Santé (ICPEES), ECPM, CNRS, UdS, 25 rue Becquerel, 67087 Strasbourg Cedex 2, France, emails: janowskai@unistra.fr (I. Janowska), dominique.begin@unistra.fr (D. Bégin)*
[e]*Department of Physics, Institute of Applied Materials, SARCHI Chair in Carbon Technology and Materials, University of Pretoria, Pretoria 0028, South Africa, email: manyalancholu@gmail.com*

Received 15 October 2016; Accepted 18 December 2016

ABSTRACT

This investigation presents the advantages and limitations of tartrazine azo dye sorption on oxygen functionalized multiwalled carbon nanotubes (O-MWCNTs) synthesized by catalytic-CVD technique in LEREC laboratory, Algeria. Our adsorbent was characterized by FESEM, HR-TEM micrographs, Raman spectroscopy, ATG, XPS and specific surface area measurements (S_{BET}). The effects of different operational parameters like contact time, initial concentration of tartrazine, adsorbent amount, pH and temperature on the sorption processes were studied in batch mode. Experiments showed that the O-MWCNT was efficient for the removal of tartrazine and the equilibrium can be reached in 60 min. The removal efficiency was found to be dependent on the initial dye concentration and there is no significant effect of temperature on the adsorption process. Also, acidic pH was found to be favorable for dye removal, while the adsorption capacity decreases with the O-MWCNTs amount. For comparison, a similar study has been performed with a commercial activated carbon (CAC) and it was found out that the functionalized MWCNT has a shorter equilibrium time and higher dye adsorption capacity than CAC, so that O-MWCNTs can be considered as potential adsorbents for dye removal from wastewater. The models of Langmuir and Freundlich isotherms are applicable to describe the process of tartrazine adsorption on the O-MWCNTs and also on the CAC conventional adsorbent.

Keywords: Multiwalled carbon nanotubes; Activated carbon; Functionalized MWNT; Specific surface area; Adsorption kinetic; Azo dye

1. Introduction

Synthetic dyes are a relatively large group of organic chemical compounds found practically in all spheres of daily life. Their world production is estimated at 700,000 ton/year of which 140,000 is discarded into effluent during the various application and manufacturing steps [1,2], which creates a real danger for environment, human and animals. Furthermore, main dyestuff wastes are known to be toxic [3], carcinogenic [4], mutagenic [5] and teratogenic [6]. Dyes are generally resistant to light, water, oxidizing agents and many chemical processes; consequently, they are difficult to be degraded once released into the aquatic systems.

Azo dyes are the largest and the most versatile class of organic dyes. They contain one or more azo bonds (–N=N–)

* Corresponding author.

as a chromophore group in association with aromatic structures containing functional groups such as –OH and –SO_3H. The complex aromatic structures of azo dyes make them more stable and more difficult to be removed from the aqueous effluents [7]. Thus, the removal of these dyes from wastewater is an important target from the environmental point of view. Tartrazine (TA) (known as E-102 or SIN-102) is one of the synthetic anionic azo dyes; it is the most commonly used substance in many industries, such as textiles, leather, paper, foodstuffs and cosmetics.

The adsorption process is an effective and attractive proposition for the treatment of the dye contaminated wastewater and can be considered as an economical alternative since it does not require any additional pre-treatment step if low-cost adsorbents are employed. A number of adsorbents, including activated carbon [8], pure multiwalled carbon nanotubes (MWCNTs) [9], acid activated red mud [10], fly ash [11], clay materials (montmorillonite [12], bentonite and zeolite [13]), biomaterials (peanut hull [14], orange peel [15] and rice husk [16]), inorganic metal oxides (ZnO [17,18], $Fe_{3-x}La_xO_4$ ferrites [19] and c-Fe_2O_3 modified TiO_2 [20]) as well as polymers [21] has been studied for dye removal. These adsorbents usually suffer from some disadvantages such as high cost, low adsorption capacity, multistep synthesis procedures or inability. Therefore, it is necessary to develop new low-cost adsorption materials with high adsorption capacity.

The discovery of carbon nanotubes (CNTs) in 1991 by Iijima [22] brought revolutionary changes into the field of nanoadsorbents during the last decades as evidenced from the huge number of paper reported in the literature. The application of carbon nanomaterials such as CNTs in the field of adsorption is one of the emerging trends for the removal of dyes from wastewater, even at very low concentrations. The nano-one-dimensional nature of the CNT, and MWNT structure, is characterized by a quite high surface area, and a relatively easy attachment of numerous chemical functional groups on their walls can be investigated (and also their decorating CNTs with nanoparticles) giving them interesting adsorption properties [23–26]. MWCNT and oxygen functionalized MWCNT (O-MWCNT) can be a real choice because of their low-cost production and their lower impact on the environment compared with SWNTs.

In this report, we investigate the adsorption process of TA as one of complicated structure dyes on the basis of the equilibrium adsorption capacity, pH effect, adsorbent dosage, ion concentrations, medium temperature and contact time. Therefore, our study focuses on TA organic pollutant adsorption on CAC and nanostructured carbon (O-MWCNT) in order to compare the efficiency of those two adsorbents.

2. Experimental procedure

2.1. Reagents and solutions

2.1.1. Macrostructured and nanostructured sorbent

The used macrostructured adsorbent support was a CAC purchased from Riedel de Haen AG, Germany. The MWCNT used as nanostructured adsorbent support was synthesized at LEREC Laboratory in Algeria by catalytic-CVD technique at 750°C using acetylene and nitrogen as, respectively, carbon source and carrier gas [27,28] using Fe_3O_4 deposited on alumina as catalyst. They were functionalized according to our previous works by an acidic treatment ($HCl:HNO_3$ = 1:3) at 80°C for 2 h and then washed and filtered using extensive deionized water until no residual acid was detected. Finally, they were dried at 100°C for 20 h.

2.1.2. Sorbate

TA (trisodium-5-hydroxy-1-(4-sulfonatophenyl)-4-(4-sulfonatophenylazo)-*H*-pyrazole-3-carboxylate) is an azo dye (CI number = 19140, EEC number = E-102) with molecular formula $C_{16}H_9N_4Na_3O_9S_2$ and molecular weight of 534.36 g/mol was obtained from Fluka and used without further purification. The structure of this dye is displayed in Fig. 1. A stock solution of 500 mg/L was prepared and working solutions with the desired concentrations were obtained by successive dilutions.

2.1.3. Analytical method

A well-known procedure for determining TA concentrations, based on Lambert–Beer law calibration plots, was applied using UV–visible spectrophotometer (Jenway 6705). The wavelength resolution and the bandwidth were, respectively, 1 and 0.5 nm. The maximum adsorption wavelength was determined equal to 428 nm. The calibration curve was then constructed. The linearization of this plot usually provided determination of the coefficient closed to 99.99%. These data were used to calculate the azo dye concentration after adsorption to determinate the sorption capacity.

2.2. Adsorption studies

Batch adsorption studies were carried out at constant temperature using a water bath. The initial concentration of TA solution was 50 mg/L for all experiments, except those carried out to determine the effect of the initial dye concentration. Each type of adsorbent was put in the contact of 100 mL of the selected dye solution, and the suspension was then vigorously agitated (the stirring speed was kept constant at 500 rpm). Flask was kept at a temperature of 25°C, except in the case for which the effect of the temperature was studied.

The experiments were performed at the pH that resulted from solving the dye in water (around 6) without further adjustment, except those conducted to examine the effect of the solution pH. Batch studies were performed as a function of both kinds of adsorbent dosage ranging from 0.0125 to

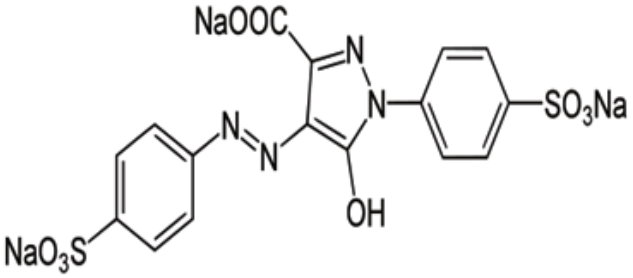

Fig. 1. Tartrazine molecule schema.

0.5 g, pH solution from 2 to 12 and adsorbate concentrations from 5 to 50 mg/L. The pH solution was adjusted using HCl (0.1 N) or NaOH (0.1 N) in separate experiments.

The amount of dye adsorbed on the surface of O-MWCNT and CAC, Q_t, expressed in milligrams of dye adsorbed per gram of carbon (mg/g) was calculated using the following relation:

$$Q_t = \frac{C_0 - C_t}{w} V \quad (1)$$

where $C_0 - C_t$ is the difference between the initial and equilibrium concentration of the dye in solution (mg/L), respectively, W is the mass of the adsorbent (mg) and V is the volume of the solution that was in contact with the adsorbent (L).

The relation between the amount of dye adsorbed on the carbon and the equilibrium concentration of the dye solution is described in the Langmuir isotherm equation.

2.3. Characterization techniques

Pristine and functionalized MWCNT were characterized using FESEM (Jeol 6700-FEG microscope) and HR-TEM (Jeol 2100F) working under an accelerated voltage of 200 kV with a point-to-point resolution of 0.23 nm in order to control the quality, structure and overall morphology of the adsorbent supports.

Raman spectroscopy was carried out on a microRaman Renishaw spectrometer (Ramascope 2000 with a spot size of 1 μm^2 and 1 cm^{-1} resolution) working with a He–Ne laser beam with 632.8 nm wavelength. The MWNT spectrum shows mainly two bands: ~1,350 cm^{-1} (D band) and ~1,576 cm^{-1} (G band). The G band originates from the Raman active E_{2g} mode explaining the in-plane atomic displacements, otherwise, the origin of D band explains the disorder features. The D/G peak intensity ratio was calculated to determine the defects to graphitic carbon ratio present in the O-MWCNT. TG analyses were carried out with a Q5000 apparatus (TA instrument) under 20 sccm airflow. The temperature was increased from room temperature to 1,000°C with a heating rate of 10°C/min.

XPS spectroscopy analyses were performed with a MultiLab 2000 (Thermo) spectrometer equipped with Al Kα anode ($h\nu$ = 1,486.6 eV) during 10 min of acquisition in order to achieve a good signal-to-noise ratio. XPS peak deconvolutions were made with the "Avantage" program from Thermoelectron Company. The C_{1s} photoelectron binding energy was set at 284.6 ± 0.2 eV relatively to the Fermi level and used as reference for calibrating the other peak positions. The XPS spectroscopy was used to examine the chemical composition of the functional groups and their concentration.

Specific area surface measurements were carried out with a TriStar (Micromeritics) sorptometer using nitrogen as adsorbent at liquid nitrogen temperature. Before measurements, the samples were systematically out-gassed at 250°C during 3 h in order to remove impurities and moisture.

Absorbance measurements were performed with a double-beam Jenway 6705 (UV–Vis) spectrophotometer (Japan) with a spectral bandwidth of 4 nm. The pH solution has been measured with a pH meter model HI 8014, Hanna Instruments (Italy).

3. Results and discussion

3.1. Adsorbents characterization

The representative low and high magnification FESEM micrographs of the tubes synthesized during 1 h by catalytic-CVD technique with a yield of 97% (ratio carbon/catalyst) are presented in Figs. 2(a)–(d). The higher magnification images clearly indicate that CNT structures are rather linear and present a high aspect ratio (length to width).

The above analyses also indicate the absence of carbon nanoparticles or other impurities in the sample, which confirms the high selectivity of the synthesis method toward CNTs formation. These MWCNTs with an average outer diameter of about 17 nm and several microns length were next treated with acid mixture in order to remove the catalysts and also to functionalize the surface of their walls with oxygen groups.

Raman spectra recorded on the MWCNT samples confirms the high crystalline graphitized structure according to Raman G peak form and the presence of some functional groups/defects/disorder according to the I_D/I_G peaks intensity ratio of about 0.8 (Fig. 3(b)). These results are in agreement with TGA results (Fig. 3(a)) where the combustion temperature was centered at around 582°C. The TGA results also confirm the high selectivity of MWCNT synthesis.

In addition, the recorded C_{1s} XPS spectrum of nanostructured MWCNTs shows the significant presence of functionalized oxygenated groups O–H, C=O and COOH (typically 6–8 wt%), respectively, as reported in Fig. 4, due to the acid purification step following the CCVD synthesis.

The specific surface area values of the O-MWCNT and CAC are 373 and 2,482 m^2/g, respectively, as shown in Table 1, and Fig. 5 indicates their pore size distribution. As can be seen, O-MWCNTs are only mesoporous (pore size > 2 nm) while activated carbons have on one hand a large microporous surface area (2,482–1,582 = 900 m^2/g) and on another hand a pore size ranged around 3 nm.

3.2. Investigations of the adsorption process

3.2.1. Effect of azo dye initial concentration

The effect of initial TA dye concentration in the range of 5–50 mg/L on adsorption efficiency using functionalized nanostructured carbon (O-MWCNT) and CAC was investigated and is reported in Fig. 6. We can observe that the removal rate from the solution increases with increasing initial concentration of TA until the adsorption reaches a dynamic equilibrium. The adsorption capacity for O-MWCNT increases from 4.39 to 79.33 mg/g as the TA concentration increases from 5 to 50 mg/g. Similarly, for CAC, it increases from 2.43 to 77.60 mg/g. A higher initial dye concentration led to the increase in the mass gradient between the liquid solution and the adsorbent, which is a driving force for the transfer of TA molecules from the bulk solution to the adsorbent surface.

However, at high initial dye concentration, dye molecules tend to aggregate or to make micelles [29–31], and this aggregation inhibits their diffusion through the adsorbent pores.

It is also noted that the adsorption rate on O-MWNT is comparable to that of CAC despite the large difference of their specific surface area. This is due to the MWCNT structure as

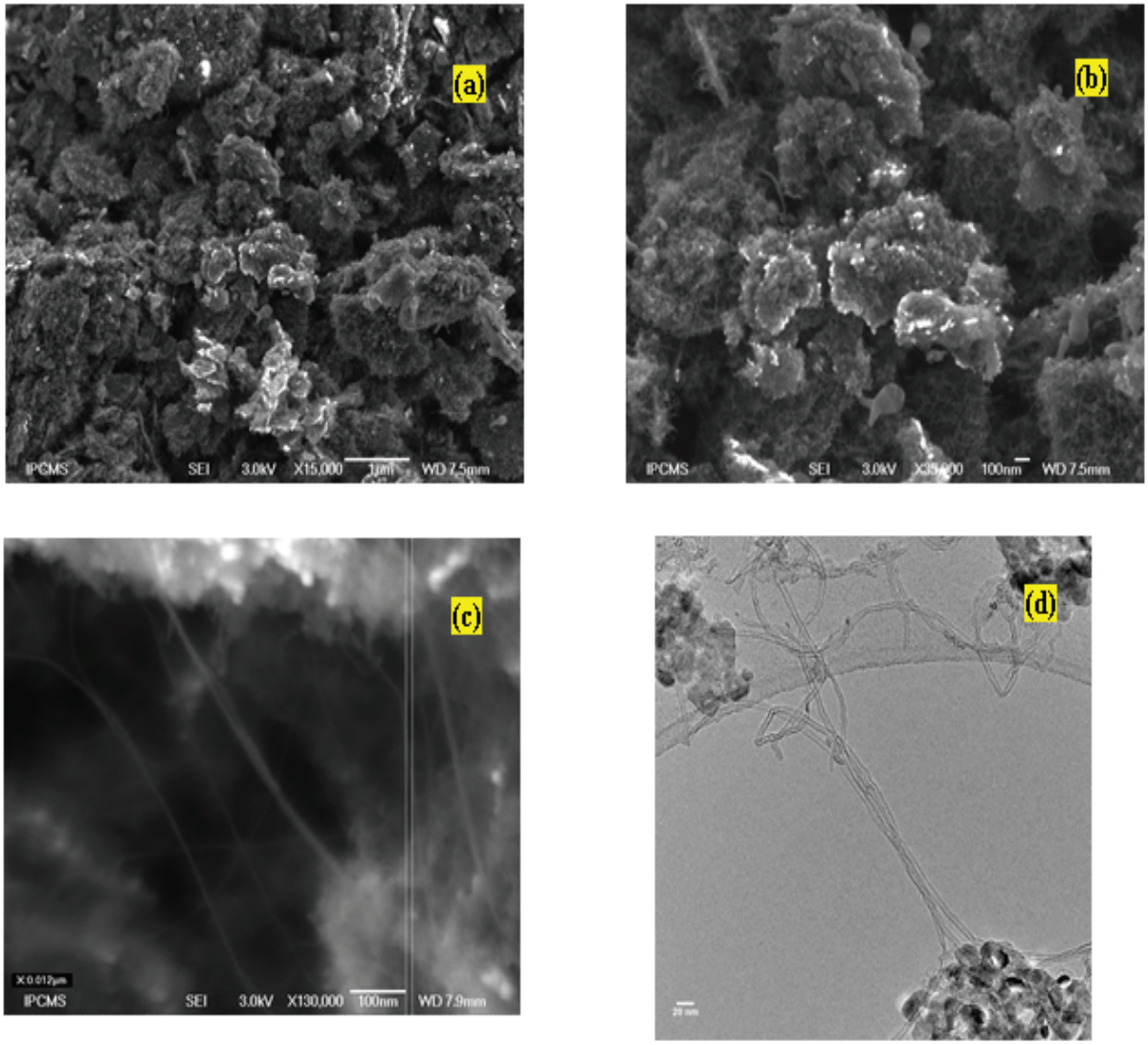

Fig. 2. Low and high magnification FESEM micrographs of: (a) and (b) pristine MWCNTs, (c) oxygen functionalized MWCNTs and (d) high resolution TEM micrograph of pristine MWCNTs.

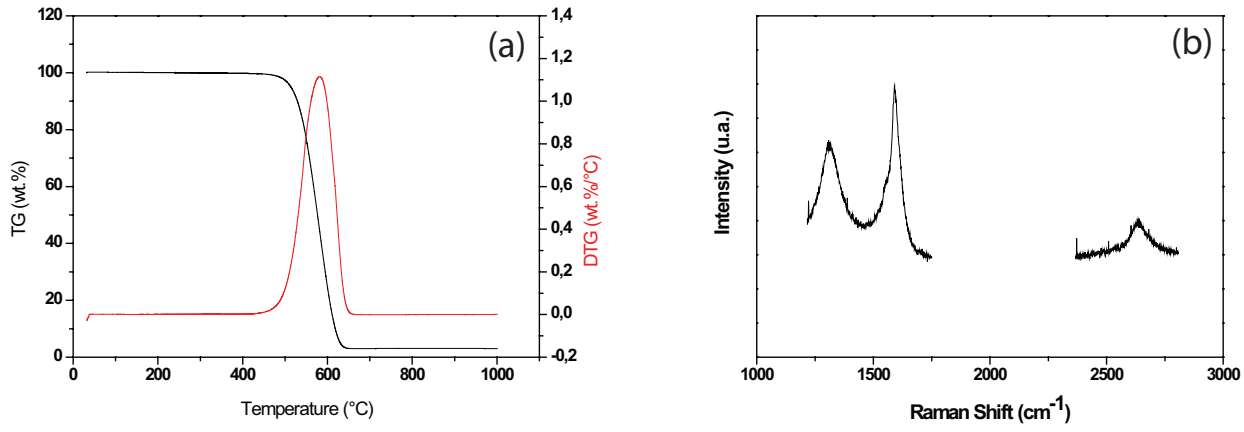

Fig. 3. (a) Thermal analysis and (b) Raman spectroscopy of oxygen functionalized MWCNT.

well as the functional groups existence and consequently the presence of different kinds of available adsorption sites on O-MWCNT such as innerwalls in tube channel and on the MWCNT surface.

Furthermore, we have also to take into account the low pore size distribution in the case of the CAC, pores which are inaccessible. It's also shown that the removal of TA was found to be fast in the initial period (less than 10 min for O-MWCNTs and 30 min for CAC) and then tends to become slow and to stabilize with increasing contact time (30–60 min for O-MWCNTs and 60–90 min for CAC). This is due to the fact that the O-MWCNTs have a "favorable" porosity compared with the CAC (higher diameter size and accessibility). The kinetic results show that the curves of contact time are single, smooth and continuous leading to equilibrium.

3.2.2. Effect of the amount of adsorbent

The mass of sorbents was varied in the range from 0.0125 to 0.5 g for the removal of TA from aqueous solution by O-MWCNTs and CAC. In these series of experiments, the concentration of TA in solution was fixed at 50 mg/L. The effect of sorbent amount on the sorption kinetics of TA is shown in Fig. 7. The amount of dye sorbed per unit mass of sorbent decreases with an increase of the sorbent amount. The increase of the sorbent amount at constant dye concentration and volume will lead to unsaturation of sorption sites through the sorption process. At higher sorbent amount to solute concentration ratios, there is a fast superficial sorption onto the sorbent surface that produces a lower solute concentration in the solution than when the sorbent to solute concentration ratio is lower. This is because a fixed mass of O-MWCNTs or CAC can only sorb a certain amount of dye.

We also note that the quantity adsorbed on the CAC ranges from 2.3 to 357.4 mg/g, while for the O-MWCNT it ranges from 4.2 to 79.5 mg/g for adsorbent mass ranging from 0.0125 to 0.5 g. This is certainly due to the high specific surface of CAC compared with the O-MWCNTs.

However, we find that the mass equal to 0.0125 g for the O-MWCNTs and 0.05 g for the CAC and we can obtain almost the same amount of adsorption 77.3 and 79.5 mg/g, respectively, for O-MWCNTs and CAC. Therefore, we took a 0.05 g CAC rate and 0.0125 g O-MWCNT rate to investigate the effect of the remaining parameters.

3.2.3. Effect of pH on the adsorption process

The pH of the solution is an important factor in the adsorption process; it governs both, the surface chemistry of the adsorbent and of the adsorbate. The effect of the pH on the uptake of TA was monitored in the pH range from 2 to 12 (Fig. 8). As shown in this figure, we can note that the removal efficiency of TA was favored in acidic solution and that it decreases from pH = 2 up to pH = 12 in the case of the O-MWCNTs. A higher adsorption capacity (88,795 mg/g) at lower pH values can be explained by the protonation properties of the adsorbent (O-MWCNT) which promotes the

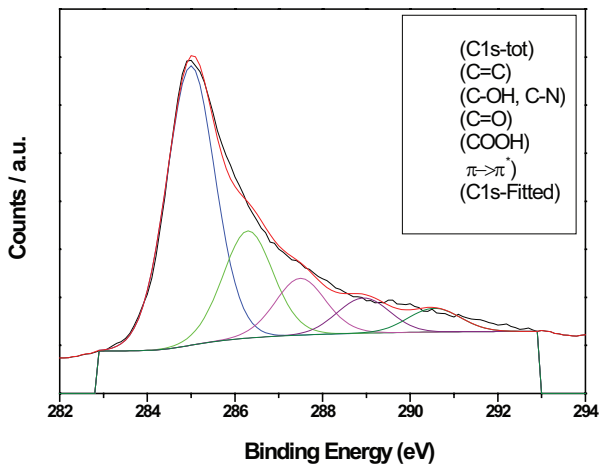

Fig. 4. C1s-XPS spectrum of O-functionalized MWCNT.

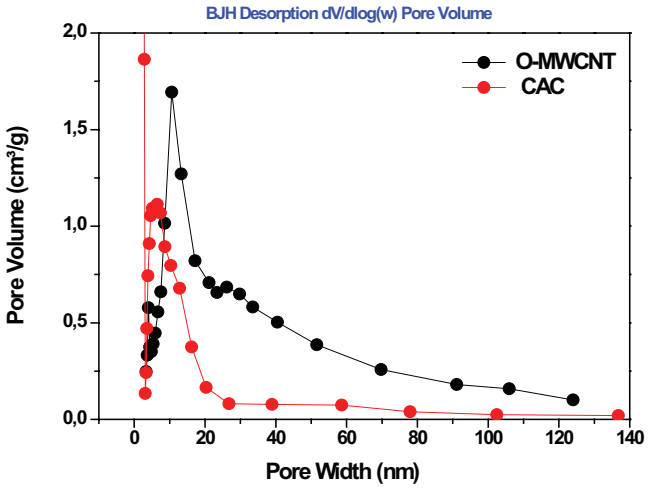

Fig. 5. Pore size distribution of O-MWCNT and CAC adsorbents.

Table 1
Specific surface area S_{BET}, pore surface area, volume and size of the adsorbent supports used in this investigation

Adsorbent supports	Specific surface area (S_{BET}) (m^2/g)	Pore surface area[a] (m^2/g)	Pore volume[b] (cm^3/g)	Pore size[c] (nm)
CAC	2,482	1,582	1.28	3.24
O-MWCNT	343	369	0.98	10.60

[a]BJH adsorption cumulative surface area of pores.
[b]BJH adsorption cumulative volume of pores between 1.7000 and 300.0000 nm diameter.
[c]BJH adsorption average pore diameter (4 V/A).

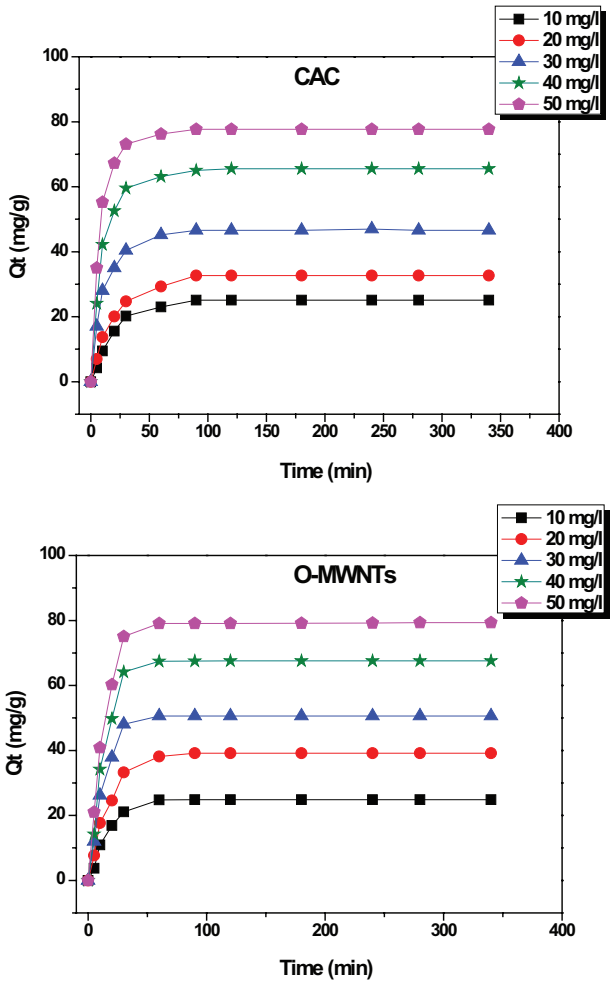

Fig. 6. Kinetics of tartrazine uptake by (left) CAC for various initial dye concentrations (conditions: sorbent dosage = 0.055 g/100 mL; stirring speed = 500 rpm; T = 25°C; pH initial) and (right) O-MWCNT for various initial dye concentrations also (conditions: sorbent dosage = 0.0125 g/100 mL; stirring speed = 500 rpm; T = 25°C; pH initial).

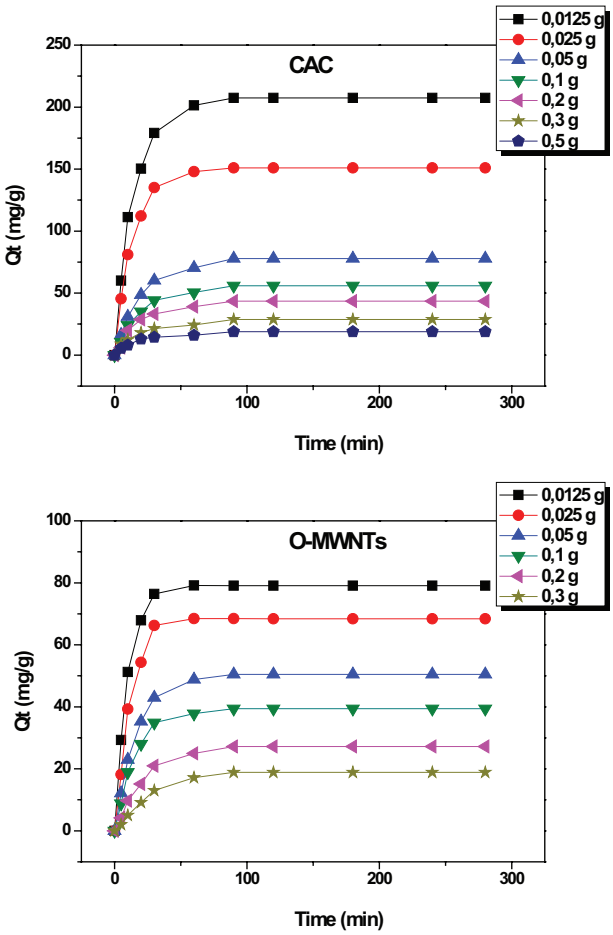

Fig. 7. Effect of the sorbent dosage on the sorption of tartrazine by (left) CAC and (right) O-MWCNTs (conditions: initial dye concentration = 50 mg/L; stirring speed = 500 rpm; T = 25°C; pH initial).

electrostatic attractions between the positive charges of the selected O-MWCNT and the negative charges of TA "anionic azo-dyes" as shown in the reaction (B):

$$X-O-H+OH^- \rightarrow X-O^- + H_2O \quad (A)$$

$$X-O-H+H^+ \rightarrow XOH_2^+ \quad (B)$$

The presence of the oxygen groups, O–H, COOH and C=O, allow also the formation of covalent bonds, hydrogen bonds and van der Waals forces. Similar relations have been reported in the literature [18,32–34]. When the pH increases, TA becomes charged positively, while the tubes are not enough charged negatively and this causes a repulsion between the adsorbent and the adsorbate (pH > pKa) which leads to the decrease of the removal rate. Whereas for the CAC, it is noted that the pH is not an important parameter to be considered during the adsorption process regarding that

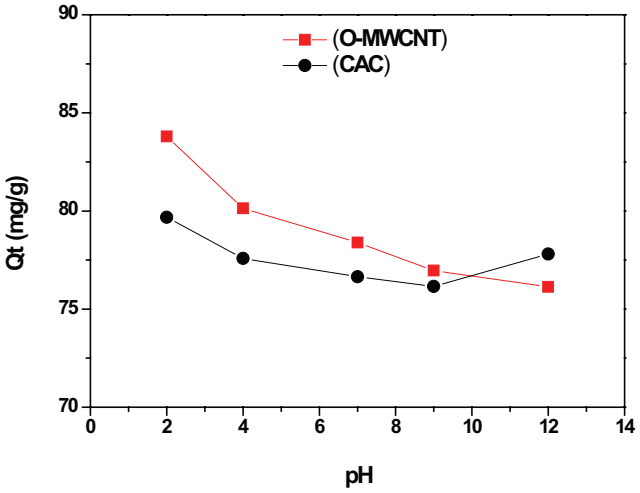

Fig. 8. pH dependence of tartrazine adsorption on two kinds of adsorbents (O-MWCNT and CAC) with initial dye concentration = 50 mg/L; O-MWCNT amount = 0.0125 g/100 mL and CAC amount = 0.05 g/100 mL; stirring speed = 500 rpm; T = 25°C.

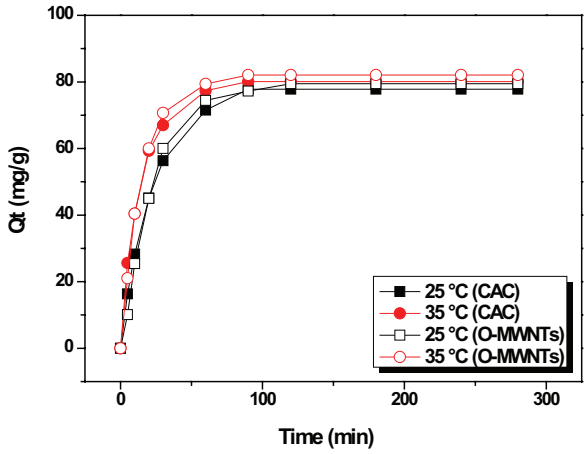

Fig. 9. Effect of the temperature on the amount of sorbed tartrazine by O-MWCNT and CAC (conditions: initial dye concentration = 50 mg/L; sorbent mass = 0.125 g for O-MWCNTs and 0.05 g for CAC (in 100 mL^{-1}); stirring speed = 500 rpm; pH initial).

it has no significant impact on the amount of adsorbed dye ($Q_{t,max}$ = 77.682 mg/g and $Q_{t,min}$ = 75.603 mg/g).

3.2.4. Effect of temperature

Fig. 9 presents the sorptive removal of TA as a function of time at two different temperatures (25°C and 35°C) on the two kinds of adsorbents. Similar shape of the kinetic curves is observed for the two temperatures and the sorption kinetics increase with increasing temperature. This indicates that the sorption process is endothermic. As it is known, the rate of diffusion of the sorbed molecules is increased with increasing the temperature, owing to the decrease of the viscosity of the solution. This enhancement is due to the acceleration of the sorption process by the increased movement of dye molecules from the bulk solution to the surface of the solid particles at higher temperatures. On the other hand, there is no significant effect of temperature on the equilibrium sorption capacity.

3.3. Adsorption isotherms

Adsorption isotherms describe how adsorbate interacts with adsorbents and the equilibrium is established between adsorbed dye on the adsorbent and the residual dye in the solution during the surface adsorption. So, the equilibrium isotherms are carried out to determine the capacity of the adsorbent as solid phase dye extraction. The sorption capacity of O-MWCNTs toward TA is found to be 80 mg/g. Consequently, we can see that the obtained amount is higher than the ones reported for most of the other adsorbents as chitin, sawdust but lower than the one for chitosan and activated carbons prepared from lignocellulosic wastes (Table 2).

The most common kinds of isotherm models describing this type of system are the Langmuir and Freundlich isotherms. The Langmuir isotherm assumes monolayer coverage of adsorbate over a homogeneous adsorbent surface. While the Freundlich isotherm superposes a heterogeneous surface with a non-uniform distribution of adsorption heat over the surface and a multilayer adsorption can be expressed [37].

Table 2
Comparison of the O-MWCNTs adsorption capacity toward tartrazine with various adsorbents cited in the literature

Adsorbent	Q_e (mg/g)	Reference
O-MWCNTs	80.00	This study
CNTs	52.24	[33]
Ag/CNTs	84.04	[33]
Nickel-doped zinc oxide	35.90	[17]
Chitin	30.00	[34]
Sawdust	4.71	[35]
Activated carbons prepared from lignocellulosic wastes	300.00	[36]
Chitosan	350.00	[34]

The Langmuir isotherms can be expressed as:

$$Q_e = Q_m\left[\frac{K_L C_e}{1+K_L C_e}\right] \quad (2)$$

where C_e is the equilibrium concentration (mg/L); Q_e is the product quantity adsorbed per unit mass of adsorbent (mg/g); Q_m is the theoretical maximum adsorption capacity (mg/g) and K_L is the thermodynamic equilibrium constant.

The Freundlich equation can be expressed as [38]:

$$\log Q_e = \log K_F + \frac{1}{n}\log C_e \quad (3)$$

where K_F and $1/n$ are Freundlich isotherm constants related to adsorption capacity and adsorption intensity, respectively. If Eq. (3) is applied, a plot of $\log Q_e$ vs. $\log C_e$ will give a straight line of slope $1/n$ and intercept K_F. The results obtained for the two type of adsorbent (O-MWCNTs and CAC) are illustrated in Fig. 10.

It is noted in Table 3 that the correlation coefficient R^2 (R^2 = 0.99) by Langmuir model is almost equal to one. This good correlation between the adsorption data and the Langmuir model indicates the homogeneous nature of the surface of the two kinds of adsorbents [39]. The maximum adsorption capacities are found to be 158.73 and 285.74 mg/g for functional O-MWCNTs and CAC, respectively. We also noted that the R_L is less than 1 ($R_L < 1$), therefore, the adsorption is favorable for both of them.

So, for Freundlich isotherms, the value of $1/n$ gives an indication of the validity of the adsorption mode in the adsorbent–adsorbate system. A value of $1/n$ between 0 and 1 indicates a favorable adsorption [40] and this indicates that the adsorption is favorable for the O-MWCNTs and CAC. Regarding also the Freundlich model, n and K_F values for the CAC adsorption is higher than those obtained with O-MWCNTs. This may indicate that the adsorption process on CAC is more favorable than in the case of O-MWCNTs; however, the affinity of the solute (TA) is substantially the same regarding that the value of $1/n$ is nearly equal (0.7384 for O-MWCNTs and 0.782 for CAC).

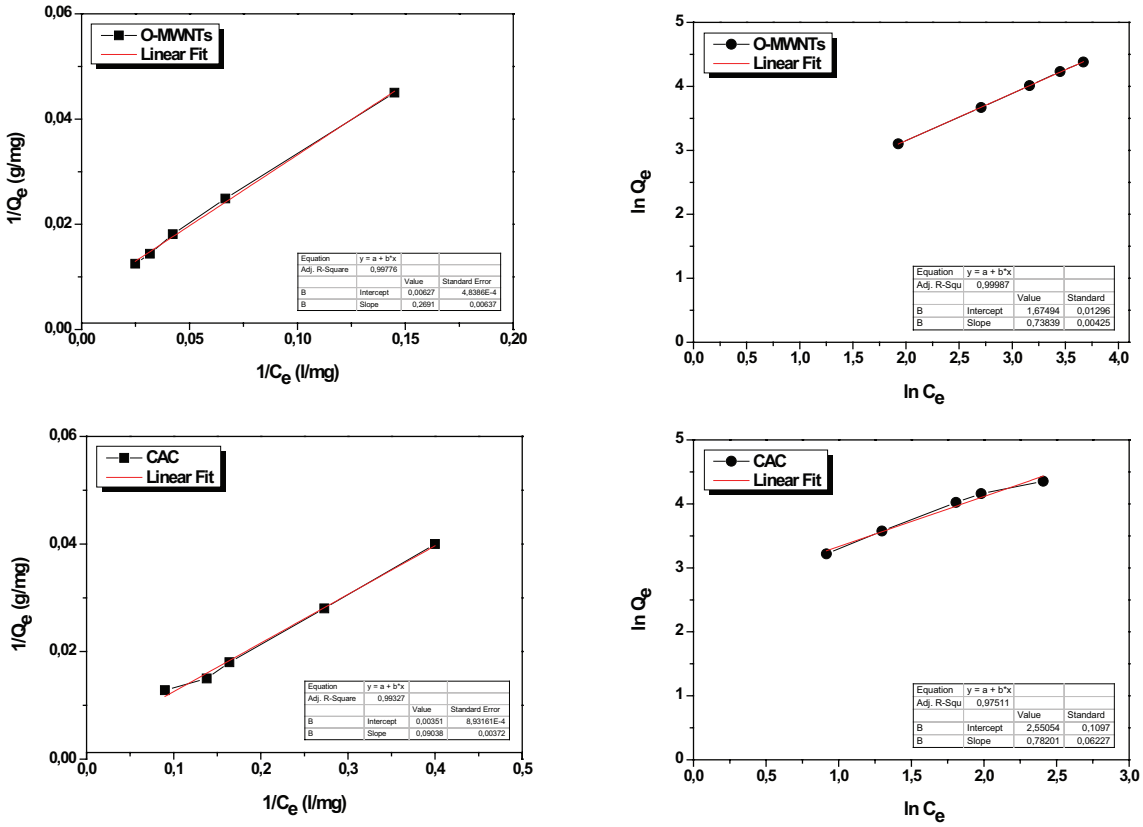

Fig. 10. Langmuir (left) and Freundlich (right) curves for O-MWCNTs and CAC.

Table 3
Isotherm parameter correlation coefficients calculated by Langmuir and Freundlich adsorption models

Parameters	Langmuir isotherm				Freundlich isotherm		
	Q_{max} (mg/g)	K_L (L/mg)	R_L	R^2	K_F	$1/n$	R^2
O-MWCNTs	158.73	0.0234	0.63	0.99776	5.3385	0.73839	0.99987
CAC	285.714	0.0387	0.508	0.99327	12.8140	0.78201	0.97511

4. Conclusions

On the basis of the above studies, the following conclusion can be drawn:

- Functionalized MWCNTs with much lower specific surface area than the CAC was found to be an alternative adsorbent to remove hazardous dyes.
- This adsorbent presents an important adsorption capacity.
- The functionalized MWCNTs have a shorter equilibrium time than activated CAC.
- The adsorption capacity is strongly dependent on the dyes concentration and the adsorbent dosage, while the temperature does not significantly affect the process.
- The pH of the solution is an important factor in the adsorption process and the acidic pH was found favorable for dyes removal on MWCNTs.
- The models of Langmuir and Freundlich isotherms are applicable to describe the process of TA adsorption on the O-MWCNTs.

Acknowledgments

The present work is in the part of a national project CNEPRU (E03420130009) financially supported by the Algerian-MHESR. The authors would like to acknowledge Th. Romero (ICPEES), D. Ihiawakrim (IPCMS), P. Bernhardt (ICPEES) and F. Antoni (InESS) for performing, respectively, FESEM, HR-TEM, XPS and Raman experiment.

References

[1] S. Sirianuntapiboon, P. Srisornsak, Removal of disperse dyes from textile wastewater using bio-sludge, Bioresour. Technol., 98 (2007) 1057–1066.
[2] P.V. Messina, P.C. Schulz, Adsorption of reactive dyes on titania-silica mesoporous materials, J. Colloid Interface Sci., 299 (2006) 305–320.
[3] M.S. Tsuboy, J.P.F. Angeli, M.S. Mantovani, S. Knasmüller, G.A. Umbuzeiro, L.R. Ribeiro, Genotoxic, mutagenic and cytotoxic effects of the commercial dye CI Disperse Blue 291 in the human hepatic cell line HepG2, Toxicol. in Vitro, 21 (2007) 1650–1655.

[4] K. Golka, S. Kopps, Z.W. Myslak, Carcinogenicity of azo colorants: Influence of solubility and bioavailability, Toxicol. Lett., 151 (2004) 203–210.
[5] K.T. Chung, Mutagenicity and carcinogenicity of aromatic amines metabolically produced from azo dyes, Environ. Carcinog. Ecotoxicol. Rev., C18 (2000) 51–74.
[6] A.R. Beaudoin, M.J. Pickering, Teratogenic activity of several synthetic compounds structurally related to trypan blue, Anat. Rec., 137 (1960) 297–305.
[7] G. Crini, Non-conventional low-cost adsorbents for dye removal: a review, Bioresour. Technol., 97 (2006) 1061–1085.
[8] M.K. Purkait, A. Maiti, S. DasGupta, S. De, Removal of congo red using activated carbon and its regeneration, J. Hazard. Mater., 145 (2007) 287–295.
[9] M. Soylak, Z. Cihan, Solid-phase extraction of tartrazine on multiwalled carbon nanotubes for separation and enrichment, 95 (2013) 559–566.
[10] A. Tor, Y. Cengeloglu, Removal of congo red from aqueous solution by adsorption onto acid activated red mud, J. Hazard. Mater., 138 (2006) 409–415.
[11] I.D. Mall, V.C. Srivastava, N.K. Agarwal, I.M. Mishra, Removal of congo red from aqueous solution by bagasse fly ash and activated carbon: kinetic study and equilibrium isotherm analyses, Chemosphere, 61 (2005) 492–501.
[12] L. Wang, A. Wang, Adsorption properties of Congo Red from aqueous solution onto surfactant-modified montmorillonite, J. Hazard. Mater., 160 (2008) 173–180.
[13] V. Vimonses, S. Lei, B. Jin, C.W.K. Chow, C. Saint, Kinetic study and equilibrium isotherm analysis of Congo Red adsorption by clay materials, Chem. Eng. J., 148 (2009) 354–364.
[14] R. Gong, M. Li, C. Yang, Y. Sun, J. Chen, Removal of cationic dyes from aqueous solution by adsorption on peanut hull, J. Hazard. Mater., 121 (2005) 247–250.
[15] C. Namasivayam, N. Muniasamy, K. Gayatri, M. Rani, K. Ranganathan, Removal of dyes from aqueous solutions by cellulosic waste orange peel, Bioresour. Technol., 57 (1996) 37–43.
[16] R. Han, D. Ding, Y. Xu, W. Zou, Y. Wang, Y. Li, L. Zou, Use of rice husk for the adsorption of congo red from aqueous solution in column mode, Bioresour. Technol., 99 (2008) 2938–2946.
[17] S. Lan, L. Liu, R. Li, Z. Leng, S. Gan, Hierarchical hollow structure ZnO: synthesis, characterization, and highly efficient adsorption/photocatalysis toward Congo red, Ind. Eng. Chem. Res., 53 (2014) 3131–3139.
[18] C. Klett, A. Barry, I. Balti, P. Lelli, F. Schoenstein, N. Jouini, Nickel doped Zinc oxide as a potential sorbent for decolorization of specific dyes, methylorange and tartrazine by adsorption process, J. Environ. Chem. Eng., 2 (2014) 914–926.
[19] L. Wang, J. Li, Y. Wang, L. Zhao, Preparation of nanocrystalline $Fe_{3-x}La_xO_4$ ferrite and their adsorption capability for Congo red, J. Hazard. Mater., 196 (2011) 342–349.
[20] M. Yu, S. Zhao, H. Wu, S. Asuha, Efficient removal of Congo red by magnetically separable mesoporous TiO_2 modified with γ-Fe_2O_3, J. Porous Mater., 20 (2013) 1353–1360.
[21] S.L. Xiao, Y.H. Li, P.J. Ma, G.H. Cui, Synthesis and characterizations of two bis(benzimidazole)-based cobaltous coordination polymers with high adsorption capacity for congo red dye, Inorg. Chem. Commun., 37 (2013) 54–58.
[22] S. Iijima, Carbon nanotubes: past, present, and future, Phys. B: Condens. Matter, 323 (2002) 1–5.
[23] D. Vairavapandian, P. Vichchulada, M.D. Lay, Preparation and modification of carbon nanotubes: review of recent advances and applications in catalysis and sensing, Anal. Chim. Acta, 626 (2008) 119–129.
[24] T.I.T. Okpalugo, P. Papakonstantinou, H. Murphy, J. McLaughlin, N.M.D. Brown, High resolution XPS characterization of chemical functionalised MWCNTs and SWCNTs, Carbon, 43 (2005) 153–161.
[25] W. Xia, Y. Wang, R. Bergsträßer, S. Kundu, M. Muhler, Surface characterization of oxygen-functionalized multi-walled carbon nanotubes by high-resolution X-ray photoelectron spectroscopy and temperature-programmed desorption, Appl. Surf. Sci., 254 (2007) 247–250.
[26] H. Zhang, N. Du, P. Wu, B. Chen, D. Yang, Functionalization of carbon nanotubes with magnetic nanoparticles: general nonaqueous synthesis and magnetic properties, Nanotechnology, 19 (2008) 315604.
[27] O. Guellati, A. Fonseca, W. Bounour, M. Guerioune, Z. Mekhalif, J. Delhalle, A. Benaldjia, J.B. Nagy, Carbon Nanotube Catalytic Deposition Synthesis, Proc. International Conference on Transparent Optical Networks "Mediterranean Winter", ICTON-MW'07, USA, 2007, pp. 1–5.
[28] O. Guellati, I. Janowska, D. Bégin, M. Guerioune, Z. Mekhalif, J. Delhalle, S. Moldovan, O. Ersen, C. Pham-Huu, Influence of ethanol in the presence of H2 on the catalytic growth of vertically aligned carbon nanotubes, Appl. Catal., A, 423–424 (2012) 7–14.
[29] T. Hihara, Y. Okada, Z. Morita, The aggregation of triphenodioxazine reactive dyes in aqueous solution and on cellulosic and nylon substrates, Dyes Pigm., 45 (2000) 131–143.
[30] Y. Zhang, J. Xiang, Y. Tang, G. Xu, W. Yan, Aggregation behaviour of two thiacarbocyanine dyes in aqueous solution, Dyes Pigm., 76 (2008) 88–93.
[31] R.K. Gautam, P.K. Gautam, S. Banerjee, Removal of tartrazine by activated carbon biosorbents of *Lantana camara*: kinetics, equilibrium modeling and spectroscopic analysis, J. Environ. Chem. Eng., 3 (2015) 79–88.
[32] A. Mittal, J. Mittal, L. Kurup, Adsorption isotherms, kinetics and column operations for the removal of hazardous dye, Tartrazine from aqueous solutions using waste materials—Bottom Ash and De-Oiled Soya, as adsorbents, J. Hazard. Mater., 136 (2006) 567–578.
[33] A. Mittal, L. Kurup, J. Mittal, Freundlich and Langmuir adsorption isotherms and kinetics for the removal of Tartrazine from aqueous solutions using hen feathers, J. Hazard. Mater., 146 (2007) 243–248.
[34] J. Goscianska, R. Pietrzak, Removal of tartrazine from aqueous solution by carbon nanotubes decorated with silver nanoparticles, Catal. Today, 249 (2015) 259–264.
[35] G.L. Dotto, M.L.G. Vieira, L.A.A. Pinto, Kinetics and mechanism of tartrazine adsorption onto chitin and chitosan, Ind. Eng. Chem. Res., 51 (2012) 6862–6868.
[36] S. Banerjee, M.C. Chattopadhyaya, Adsorption characteristics for the removal of a toxic dye, tartrazine from aqueous solutions by a low cost agricultural by-product, Arab. J. Chem., (2013). doi: http://dx.doi.org/10.1016/j.arabjc.2013.06.005.
[37] H. Freundlish, Uber die adsorption in Losungen, J. Phys. Chem., 57 (1906) 385–470.
[38] G. Durán-Jiménez, V. Hernández-Montoya, M.A. Montes-Morán, A. Bonilla-Petriciolet, N.A. Rangel-Vázquez, Adsorption of dyes with different molecular properties on activated carbons prepared from lignocellulosic wastes by Taguchi method, Microporous Mesoporous Mater., 199 (2014) 99–107.
[39] B. Karagozoglu, M. Tasdemir, E. Demirbas, M. Kobya, The adsorption of basic dye (Astrazon Blue FGRL) from aqueous solutions onto sepiolite, fly ash and apricot shell activated carbon: kinetic and equilibrium studies, J. Hazard. Mater., 147 (2007) 297–306.
[40] C.H. Weng, Y.F. Pan, Adsorption of a cationic dye (methylene blue) onto spent activated clay, J. Hazard. Mater., 144 (2007) 355–362.